Journal of Innate Immunity

Research Article

J Innate Immun 2023;15:647–664
DOI: 10.1159/000532063

Received: August 21, 2022
Accepted: July 11, 2023
Published online: August 22, 2023

MicroRNA-9-1 Attenuates Influenza A Virus Replication via Targeting Tankyrase 1

Gayan Bamunuarachchi[a, b] Kishore Vaddadi[a, b] Xiaoyun Yang[a, b] Quanjin Dang[a, b] Zhengyu Zhu[a, b] Sankha Hewawasam[a, b] Chaoqun Huang[a, b] Yurong Liang[a, b] Yujie Guo[a, b] Lin Liu[a, b]

[a]Oklahoma Center for Respiratory and Infectious Diseases, Oklahoma State University, Stillwater, OK, USA; [b]Lundberg-Kienlen Lung Biology and Toxicology Laboratory, Department of Physiological Sciences, Oklahoma State University, Stillwater, OK, USA

Keywords
MicroRNA · Poly(ADP-ribose) polymerase · Influenza virus · Type I interferon

Abstract
An unstable influenza genome leads to the virus resistance to antiviral drugs that target viral proteins. Thus, identification of host factors essential for virus replication may pave the way to develop novel antiviral therapies. In this study, we investigated the roles of the poly(ADP-ribose) polymerase enzyme, tankyrase 1 (TNKS1), and the endogenous small noncoding RNA, miR-9-1, in influenza A virus (IAV) infection. Increased expression of TNKS1 was observed in IAV-infected human lung epithelial cells and mouse lungs. TNKS1 knockdown by RNA interference repressed influenza viral replication. A screen using TNKS1 3′-untranslation region (3′-UTR) reporter assays and predicted microRNAs identified that miR-9-1 targeted TNKS1. Overexpression of miR-9-1 reduced influenza viral replication in lung epithelial cells as measured by viral mRNA and protein levels as well as virus production. miR-9-1 induced type I interferon production and enhanced the phosphorylation of STAT1 in cell culture. The ectopic expression of miR-9-1 in the lungs of mice by using an adenoviral viral vector enhanced type I interferon response, inhibited viral replication, and reduced susceptibility to IAV infection. Our results indicate that miR-9-1 is an anti-influenza microRNA that targets TNKS1 and enhances cellular antiviral state.

Introduction

Influenza A viruse (IAV) can infect humans and animals and is highly transmissible both within and between host species. IAV infects the human respiratory tract and lead to respiratory infections, which can cause both seasonal and unpredictable pandemics. Even though IAV circulates year-round, IAV infections are the most common in the cold half of the year. IAV infection in infants, the elderly, and people with chronic respiratory diseases has a high mortality rate. The Centers for Disease Control and Prevention (CDC) estimated that influenza-associated illness in the USA ranges between 9 and 45 million with 12,000–61,000 deaths annually since 2010 [1].

karger@karger.com
www.karger.com/jin

Correspondence to:
Lin Liu, lin.liu@okstate.edu

An outbreak of fatal respiratory pandemic diseases can cause a significant social and economic impact globally. During the first known influenza pandemic occurred in 1918 (Spanish Flu), approximately one-third of the world's population became infected with the virus [2]. Since then, several influenza pandemics emerged with the most recent one in 2009.

Influenza viruses are classified into four types: A, B, C, and D. Human influenza A and B viruses account for most of the seasonal infections. Between them, IAV causes the highest number of hospitalized cases worldwide. Influenza C virus infections generally cause mild influenza-like illness and are not thought to cause human influenza epidemics. Influenza D virus primarily infects cattle and pigs and is not a human pathogen [3]. Viral ribonucleoprotein (RNP) complex contains RNA-dependent RNA polymerase that helps viral genome replication. However, this process is highly error-prone and thus leads to frequent mutations that evade immune responses [4]. Even though our understanding of the influenza virus biology and pathogenesis is greatly improved in past decades, our knowledge of the host immune response and viral evasion need to be expanded.

The seasonal influenza vaccine is mainly based on annual predictions and thus has several limitations that reduce efficacy. Antivirals against influenza have been developed for a long time to reduce the viral burden. There are two classes of antivirals, matrix protein 2 (M2) ion channel blockers (rimantadine and amantadine) and neuraminidase (NA) inhibitors (oseltamivir, zanamivir, and peramivir), that have been approved by the US Food and Drug Administration (FDA) to treat influenza. Most recently, the influenza polymerase inhibitor, baloxavir marboxil, was added to the regimen of antiviral drugs to combat influenza infection [5]. All the anti-influenza drugs target viral proteins, which leads to drug resistance. Rimantadine and amantadine are no longer recommended for use due to the emergence of resistance [5]. The influenza virus relies on host cellular functions for its efficient replication. Thus, potential therapeutics that target host factors to reduce viral burden would be an alternative solution to overcome drug resistance [6].

The poly (ADP-ribose) polymerases (PARPs), also known as Diphtheria toxin-like ADP-ribosyltransferases (ARTDs), are a family of proteins that catalyze the enzymatic activity of transferring of ADP-ribose motifs to target proteins. The PARP family contains 17 members with 5 poly(ADP-ribose) polymerases, 10 mono(ADP-ribose) polymerases, and 2 being catalytically inactive [7, 8]. PARPs are involved in many cellular processes, including DNA replication, recombination, and repair, modulation of chromatin structure, and transcription. PARPs are also associated with the interferon response and antiviral defense [8–11]. Some PARPs induce type I interferon (IFN) responses. For example, PARP1 promotes the degradation of type I IFN receptor 1 via its interaction with viral hemagglutinin [12]. PARP13 (also called ZAPS) activates RIG-1 by interacting and enhancing RIG-1 oligomerization [13]. PARP9 interacts with STAT1 to induce its nuclear translocation [14]. PARPs have also been shown to exert its antiviral activities by binding viral RNAs and proteins [15–17].

Tankyrase (TNKS) or PARP5 have two isoforms, TNKS1 or PARP5a and TNKS2 or PARP5b. Both isoforms consist of an N-terminal ankyrin domain, a sterile alpha module (SAM) domain, and the C-terminal PARP catalytic domain. TNKS1 has a distinct N-terminal proline and serine rich (HPS) domain, which is absent in TNKS2 [18]. TNKS has been implicated in the regulation of telomere length, cancer progression, lung fibrogenesis, and myelination [18]. Moreover, TNKS is involved in viral infection including human cytomegalovirus (HCMV), Epstein-Barr virus, and herpes simplex virus (HSV) [19–22]. HCMV inhibits PARsylation of TNKS and the Wnt/β-catenin signaling, which results in enhanced HCMV replication [19, 21]. TNKS1 reduces Epstein-Barr virus replication by directly binding the viral protein, EBNA1 [20]. HSV utilizes TNKS1 for its replication via modulating host ERK signaling and its interaction with viral protein, ICP0 [22]. We have recently shown that TNKS2 is a proviral host factor for influenza virus [23]. However, whether TNKS1 regulates IAV replication is unclear.

MicroRNAs (miRNAs) are a class of small (~22 nt) endogenous noncoding RNAs that play an important role in regulating influenza virus replication [24]. A miRNA possesses a short nucleotide sequence known as "seed sequence" that binds the complementary binding site in the 3′-untranslated region (3′-UTR) of mRNA to cause mRNA degradation and translational repression [25]. IAV alters the expression of host miRNAs [26–28]. miRNAs can be upregulated or downregulated by IAV mainly through altered host signaling [24]. For example, miR-1290 is upregulated by IAV-induced ERK pathway [29]. miR-203 is induced by DNA demethylation of its promoter upon IAV infection [30]. On the other hand, cellular miRNAs regulate antiviral innate immunity and other defense systems against IAV infection [27, 28, 30–36].

miR-9 is a highly conserved miRNA among 22 vertebrate species [37]. There are 3 isoforms in humans: has-miR-9-1, has-miR-9-2, and has-miR-9-3 that are located

on chromosome 1, 5, and 15, respectively [38]. miR-9 is an important regulator of development, neurodegenerative diseases, and cancer [37]. Among the 3 human miR-9 precursors, has-miR-9-1 is specifically upregulated by the activation of toll-like receptor 4 using lipopolysaccharides [39]. miR-9 is also upregulated in the Zika virus-infected mice, which is associated with the development of microcephaly [40]. miR-9 is involved in influenza virus infection by targeting chemoattractant protein 1-induced protein 1 in cell culture [41].

Host innate immunity represents the critical initial barrier that viruses need to overcome for its efficient replication in order to invade a host. Interferons (IFNs) play a central role in establishing an antiviral state in nonimmune cells and elicit antiviral innate immunity against viral infections [42]. Both type I IFNs (IFNα and IFNβ) and type III IFNs (IFNλ) participate in limiting influenza replication in epithelial cells [3, 43]. miRNAs have abilities to control IFN responses during viral infection by targeting host factors [44, 45]. Some miRNAs also act as ligands to initiate the type I IFN response during IAV infections [28].

The purposes of this study were to (1) determine whether IAV regulates TNKS1 expression and vice versa and (2) identify miRNAs that target TNKS1 and investigate associated molecular mechanisms. We found that TNKS1 expression was upregulated during IAV infection, and knockdown of TNKS1 attenuated IAV replication. TNKS1 is a target of miR-9-1, which inhibits IAV infection by enhancing antiviral innate immunity.

Materials and Methods

Cells and Viruses

Human embryonic kidney (HEK293 and HEK293T), Madin-Darby canine kidney epithelial (MDCK), human lung epithelial (A549) cells, and Vero cells were obtained from the American Type Culture Collection (ATCC, Manassas, VA, USA). Human primary bronchial tracheal epithelial cells (HBTEC) were purchased from Lifeline Cell Technology (Frederick, MD, USA). MDCK, Vero, and HEK cells were cultured in T-75 flasks (Thermo Fisher Scientific, Waltham, MA, USA) with DMEM media containing 10% fetal bovine serum (FBS) and 1% penicillin and streptomycin (PS). A549 cells were maintained in F12K medium with 10% FBS and 1% PS. HBTEC cells were cultured in BronchiaLife™ Complete Medium (Lifeline Cell Technology, Cat # LL-0023), and these cells were used up to passage 8.

Influenza virus H1N1 A/PuertoRico/8/34 (A/PR/8/34) strain was purchased from ATCC. H1N1 A/Oklahoma/3052/2009 (pdm/OK/09), H1N1 A/WSN/1933 (A/WSN/33), and H3N2 A/Oklahoma/309/2006 (A/OK/309/06) strains were kindly provided by Dr. Gillian Air (University of Oklahoma Health Sciences Center). 10-day-old specific-pathogen-free embryonated chicken eggs (Charles River Laboratories, Norwich, CT, USA) were used for the virus propagation. Once inoculated with the virus, the eggs were incubated at 35°C for 3 days. The allantoic fluid harvested from the infected eggs was centrifuged at 2,000 *g* for 10 min, aliquoted, and stored at −80°C.

Construction of Vectors

Lentiviral short hairpin RNA (shRNA) vectors were constructed as previously described [46]. A shRNA of human TNKS1 (online suppl. Table 1; for all online suppl. material, see https://doi.org/10.1159/000532063) was cloned into a lentiviral pmiRZip vector (Cat # MZIPxxxPA-1, System Biosciences, Mountain View, CA, USA). A scrambled shRNA (shCon) was inserted into the same vector and used as a control.

miRNA expression vectors were constructed as previously described [46]. The mature miRNA sequences along with their flanking sequences (~200 bp at each end) were amplified from human genomic DNA by PCR using specific pairs of primers (online suppl. Table 1). PCR products were cloned into a pENTR vector between EGFP and VS40 poly-A terminal sequence through EcoR I and Xho I sites. The miRNA inserts in the pENTR vector were switched into an adenoviral vector by the Gateway technique (Invitrogen, Carlsbad, CA, USA) for the production of adenoviruses. The miRNA PCR products were also cloned into a modified pLVX-Puro lentiviral vector that uses CMV promoter to drive EGFP-miRNA expression (Clontech, Mountain View, CA, USA) for making lentivirus. A random genomic DNA with a similar size and without any stem-loop structures or miRNA sequences was inserted into the pENTR vector or pLVX-Puro lentiviral vector and used as the controls (miR-Con).

3′-UTR luciferase reporter vectors were constructed as previously described [46]. A primer pair listed in online supplementary Table 1 was used to amplify the 3′-UTR of human TNKS1 by PCR using human genomic DNA. The mutants carrying mutated miR-9-5p or miR-9-3p binding sites were created through overlap PCR using primers listed in online supplementary Table 1. PCR products were inserted into the pmirGLO Dual-Luciferase (Firefly and *Renilla*) miRNA target expression vector (Promega, Madison, WI, USA) through NheI and SalI restriction sites. TNKS2 3′-UTR luciferase reporter vector was created in the previous publication [23]. TNKS1 overexpression vector (pLSJH-TNKS1) was kindly provided by Drs. Amit Bhardwaji and Susan Smith (New York University School of Medicine) [47].

Lentivirus and Adenovirus Production

Lentivirus and adenovirus were prepared as previously described [46]. To make a lentivirus, pmiRZip-shTNKS1 or pLVX-CMV-EGFP-miR-9-1 plasmid was co-transfected into HEK293T cells along with psPAX2 and pMD2G plasmids (Addgene, Cambridge, MA, USA) using 6 μg polyethylenimine (PEI)/μg plasmids. The lentiviruses in the culture media were harvested, and titers were determined in HEK293T cells. Virus aliquots were stored at −80°C.

To make an adenovirus, an adenoviral vector expressing miR-9-1 or miR-Con was transfected into HEK293A cells. The crude viral lysate was frozen/thawed 3 times to release the virus. After centrifugation at 1,500 rpm for 10 min, the virus in supernatant was purified and concentrated using the Adeno-X Maxi purification kit (Clontech). Adenoviral titer was determined in HEK293A cells, and viral aliquots were stored at −80°C.

miRNA Overexpression

For overexpressing miRNAs in HEK293 cells, the cells were seeded in a 12-well plate at a density of 4×10^5 cells/well, transfected with a miRNA expression pENTR plasmid or its control plasmid, miR-Con (1.25 μg per well) using Lipofectamine 3,000 (Thermo Fisher Scientific), and cultured for 24 h. For overexpressing miRNAs in A549 cells, the cells were seeded in a 12-well plate at a density of 2×10^5 cells/well and transduced with a lentivirus expressing miRNA or its control, miR-Con at a multiplicity of infection (MOI) of 100 in the presence of polybrene (Sigma-Aldrich, St. Louis, MO, USA, 10 μg/mL) for 48 h.

Influenza Virus Infection

A549 and Vero cells cultured in normal plates or HEK293 cells cultured in collagen type I-coated wells were washed with phosphate-buffered saline (PBS) and inoculated with influenza virus at various MOIs in a serum-free medium for 1 hr. The inoculation media were removed and replaced with serum-free media supplemented with 0.3% bovine serum albumin and 0.5 μg/mL L-(tosylamide-2-phenyl) ethyl chloromethyl ketone-treated trypsin (TPCK-trypsin) (Worthington Biochemical Corporation, Lakewood, NJ, USA). The cells were cultured for different times and used for determining viral mRNA and protein levels, and the media were used for determining progeny virus production.

RNA Isolation and Real-Time PCR

The quantitation of mRNAs and miRNAs were performed as previously described [35]. Total RNAs were isolated using TRI Reagent (Molecular Research Center, Cincinnati, OH, USA). One μg of RNAs was treated with RNase-Free DNase I (Thermo Fisher Scientific) and reverse-transcribed into cDNAs by using oligo (dT), random primers, and Moloney murine leukemia virus reverse transcriptase (Promega). For measuring miRNA levels, Poly-A tails were added to RNAs using *E. coli* poly(A) polymerase (New England Biolabs, Ipswich, MA, USA), and then the RNAs were reverse-transcribed into cDNAs using Poly-T-Adaptor (New England Biolabs) and Moloney murine leukemia virus reverse transcriptase. Real-time PCR was performed in a 20-μL reaction containing gene- or miRNA-specific primers listed online supplementary Table 2 and SYBR Green PCR master mix (Eurogentec, Fremont, CA, USA). PCR was carried out on ABI 7500 real-time PCR System (Applied Biosystems, Foster City, CA, USA) using cycling conditions: 95°C for 1 min, followed by 40 cycles of 95°C for 15 s and 60°C for 1 min. β-actin and U6 were used as internal controls for mRNAs and miRNAs, respectively. The expression level of a mRNA and miRNA relative to the housekeeping gene was calculated using the comparative Ct method.

Plaque Assay

Virus titers were determined by the plaque assay as previously described [48]. MDCK cells (1.5×10^5/well) were seeded in 12-well plates. After a 24-h culture, cells were washed with sterile PBS and infected with a series of ten-fold dilutions of virus stocks in a serum-free medium containing 1 μg/mL TPCK-trypsin. Cells were incubated for 1 h at 37°C. Simultaneously, 2x DMEM media containing 2 μg/mL TPCK-trypsin and 2% heated SeaPlaque agarose were incubated in a 37°C water bath. Virus inoculums were aspirated, and 2 mL of overlay media (1:1 ratio of 2x DMEM media containing 2 μg/mL TPCK-trypsin and 2% SeaPlaque agarose) were added to each well. After agarose was solidified, plates were incubated upside down in a 37°C incubator with 5% CO_2 atmosphere for 48–72 h. After plaque formation, cells were fixed with 10% formaldehyde solution for 30 min, and semisolid overlay media plugs were removed. For staining, cells were covered with a minimal amount of crystal violet solution (Sigma) for 10 min and then washed off the excess staining solution. Dried plates were used to determine the virus titers.

Western Blotting

Western blot analysis was performed as previously described [35]. Total proteins were separated on 10% sodium dodecyl sulfate-polyacrylamide gel electrophoresis and transferred to nitrocellulose membrane. Membranes were blocked with 5% skimmed milk in 1× Tris-buffered saline with 0.1% Tween-20 (TTBS) for 1 h and incubated with overnight with the following primary antibodies: rabbit anti-TNKS1 (1:1,000, A302-399A, Bethyl Laboratories, Montgomery, TX, USA), mouse anti-NP (1:50, HB-65, ATCC), mouse anti-NS1 (1:1,000, sc-130568, Santa Cruz, Dallas, TX, USA), rabbit anti-p-Stat1 (1:1,000, CS-9167S, Cell Signaling), rabbit anti-Stat1 (1:1,000, CS-14994S, Cell Signaling), mouse anti-flag (1:1,000, #8146, Cell Signaling), rabbit anti-MAVS (1:1,000, #3993, Cell Signaling) and mouse anti-β-actin (1:1,000, MA5-11869, Thermo Fisher Scientific). After being incubated with primary antibodies, nitrocellulose membranes were incubated with horseradish peroxidase-conjugated goat anti-rabbit or goat anti-mouse (1:1,000) secondary antibodies for 1 h. The protein bands were visualized using the SuperSignal™ West Pico PLUS chemiluminescent substrate (Thermo Fisher Scientific).

Enzyme-Link Immunosorbent Assay

IFNβ production in the culture media of IAV-infected HEK293 and A549 cells was determined by using VeriKine™ human IFN beta sandwich enzyme-link immunosorbent assay (ELISA) Kit (PBL Assay Science, Piscataway, NJ, USA). Briefly, precoated microtiter strips were incubated with 50 μL of IFNβ standards, blanks, and samples. After a 1-h incubation, the microtiter strips were washed with washing buffer and 100 μL antibody solution was added. After an additional 1-h incubation, the strips were washed and incubated with 100 μL horseradish peroxidase-conjugated secondary antibodies for 1 h at room temperature. The strips were washed and treated with tetramethylbenzidine substrate solution for 15 min in dark. The reaction was terminated by the addition of 100 μL stop solution, and the absorbance was read at 450 nm using a microplate reader (Bio-Rad, Hercules, CA, USA). The amount of IFNβ in the samples was derived from the standard curve. T1-α levels in the bronchoalveolar lavage fluid (BALF) were measured by using the Podoplanin ELISA Kit (MyBioSource, San Diego, CA, USA) according to the manufacturer's instructions.

Dual-Luciferase Assay

For 3′-UTR reporter assay, A549 cells were seeded in a 96-well plate (1×10^4 cells/well) for 24 h. Cells were co-transfected with a pENTR miRNA expression plasmid or its control (miR-Con) (100 ng) and 5 ng of pmirGLO-firefly-TNKS1-3′-UTR, its mutant or pmirGLO-firefly-TNKS2-3′-UTR vector by using Lipofectamine 3000 (Invitrogen) for 24 h. Cells were lysed by using passive lysis buffer (40 μL) and centrifuged (4°C) at 12,000 *g* for 5 min. Next, the supernatant (10 μL) was taken for the reporter assay by using

the Dual-Luciferase Assay System Kit (Promega, Madison, WI, USA). Dual luciferase activities were measured by FLUOstar OPTIMA microplate fluorometer (BMG LABTECH, Offenburg, Germany). Firefly luciferase activities were normalized to *Renilla* luciferase activities.

For influenza virus reporter assay [49], A549 and HEK293 cells were seeded into 96-well plates (1×10^6 cells/plate). Cells were co-transfected with a pENTR miRNA or a miR-Con expression plasmid (100 ng), an influenza A luciferase reporter vector, NP-UTR-Luc (20 ng), and a pRL-TK *Renilla* luciferase vector (20 ng) for 24 h. After transfection, the cells were infected with H1N1 A/PR/8/34, H1N1 A/WSN/33, H1N1 pdm/OK/09, H3N2 A/OK/309/06 at an indicated MOI for 48 h. Cells were lysed with passive lysis buffer, and dual luciferase activities were measured as described above.

For interferon-stimulated response element (ISRE) reporter assay, 50 ng of ISRE luciferase reporter plasmid (QIAGEN, Germantown, MD, USA), 100 ng of pENTR miRNA or miR-Con expression plasmid, and 10 ng of pRL-TK *Renilla* luciferase plasmid (QIAGEN) were transfected into HEK293 cells for 24 h. Afterward, cells were infected with H1N1 A/PR/8/34 virus at an MOI of 0.01 for 48 h, and dual luciferase activities were measured as described above.

Animal Studies

Male and female C57BL/6J mice (8–9 weeks old) were purchased from Jackson Laboratory (Bar Harbor, ME, USA). Adenovirus expressing miR-Con (Ad-miR-Con) or miR-9-1 (Ad-miR-9-1) (1×10^9 infectious unit in 50 μL) was intratracheally delivered into the lungs of male and female mice under anesthesia. Two days after, mice were infected intranasally with H1N1 A/PR/8/34 (160 plagues forming unit [PFU] in 50 μL). Mice were euthanized at 0, 3, or 7 days postinfection (dpi). 10% neutral buffered formalin (Thermo Fisher Scientific) was used to fix the left lungs for immunostaining. The right lungs were lavaged 3 times with 0.5 mL of PBS, and the right lung tissues were snap-frozen in liquid nitrogen. Under liquid nitrogen, by using mortar and pestle, the right lungs were powdered and aliquoted into 3 fractions and stored at −80°C for further use. One aliquot of lung tissue (volume adjusted to weight) was dissolved in DMEM medium, subjected to 3 cycles of freeze and thaw, and used for virus titer determination by plaque assay. Another aliquot was lysed in tissue lysis buffer with 30x Halt™ Protease and Phosphatase Inhibitor Cocktail (Thermo Fisher Scientific) for Western blot analysis. The remaining aliquot was dissolved in TRI Reagents for RNA isolation and real-time PCR analysis.

For survival studies, female C57BL/6J mice (8–9 weeks old) were treated with the same dose of Ad-miR-9-1 or Ad-miR-Con adenovirus virus at −2 dpi as described above and infected with 1x mouse lethal dose 50 (MLD50) of H1N1 A/PR/8/34. Mice were observed for clinical signs and body weight loss daily. Clinical scores were assessed as previously described [23].

Data Analysis

For in vitro studies, a minimum of three independent experiments were performed. For in vivo studies, at least six animals per group were used. Graph Pad Prism version 7.0 was used for statistical analysis. Student's *t* test and one-way or two-way ANOVA, followed by post hoc comparisons, were used to compare two groups or multiple groups, respectively. A p value of <0.05 was considered significant.

Results

Influenza Virus Increases TNKS1 mRNA and Protein Levels

TNKS1/2 expression was induced during HCMV infection [21]. Another study found that the expression of TNKS1, but not TNKS2, was suppressed by HSV infection [22]. These previous studies suggest that TNKS1 and 2 may respond to virus infections differently. We thus studied whether IAV infection alters TNKS1 expression. A549 lung epithelial cells were infected with H1N1 A/PR/8/34 at an MOI of 0.01 and collected at 24, 48, and 72 h. Western blot analysis showed that viral NP protein was detected starting from 24 h postinfection (hpi) and further increased at 48 and 72 hpi, indicating efficient IAV infection (Fig. 1a, b). TNKS1 protein levels were steadily increased during IAV infection. Moreover, TNKS1 mRNA levels were also induced by IAV in a dose- and time-dependent manner (Fig. 1c, d). Additionally, TNKS1 mRNA and protein levels were increased similarly in HEK293 cells infected with IAV (online suppl. Fig. 1A–C).

We next examined the TNKS1 expression in response to different strains of IAV. We chose two commonly used laboratory strains, H1N1 A/PR/8/34 and H1N1 A/WSN/1933, and two clinical isolates of H3N2 A/OK/309/2006 and 2009 pandemic strain, H1N1 A/OK/3052/2009. TNKS1 mRNA expression was increased in the infected A549 cells with all the strains tested (Fig. 1e). Furthermore, TNKS1 protein expression was also elevated in the lung tissues of mice infected with A/PR/8/34 (Fig. 1f, g). Together, these studies suggest that TNKS1 protein expression was induced by IAV in vitro and in vivo.

Knockdown of TNKS1 Restricts IAV Replication

To evaluate the role of TNKS1 in IAV infection, we constructed two shRNA vectors to reduce TNKS1 levels. HEK293 cells were transfected with a TNKS1 shRNA vector (shTNKS1) or a control vector (shCon) and infected with H1N1 A/PR/8/34 at an MOI of 0.01 for 48 h. shTNKS1-1 and shTNKS1-2 reduced the TNKS1 protein levels to 53 ± 11% and 58 ± 17% of that of shCon, respectively (Fig. 2a, b). Both TNKS1 shRNAs reduced the viral NP and NS1 protein expression compared to shCon. Moreover, the virus titer was repressed by shTNKS1-1 and shTNKS1-2 (Fig. 2c). These results demonstrate that the knockdown of TNKS1 expression attenuates IAV replication.

Screening of miRNAs that Target TNKS1 with Anti-Influenza Activities

Small interfering RNAs (siRNAs) and miRNAs have an important role in gene regulation and already have reached clinical trials to treat human diseases [50].

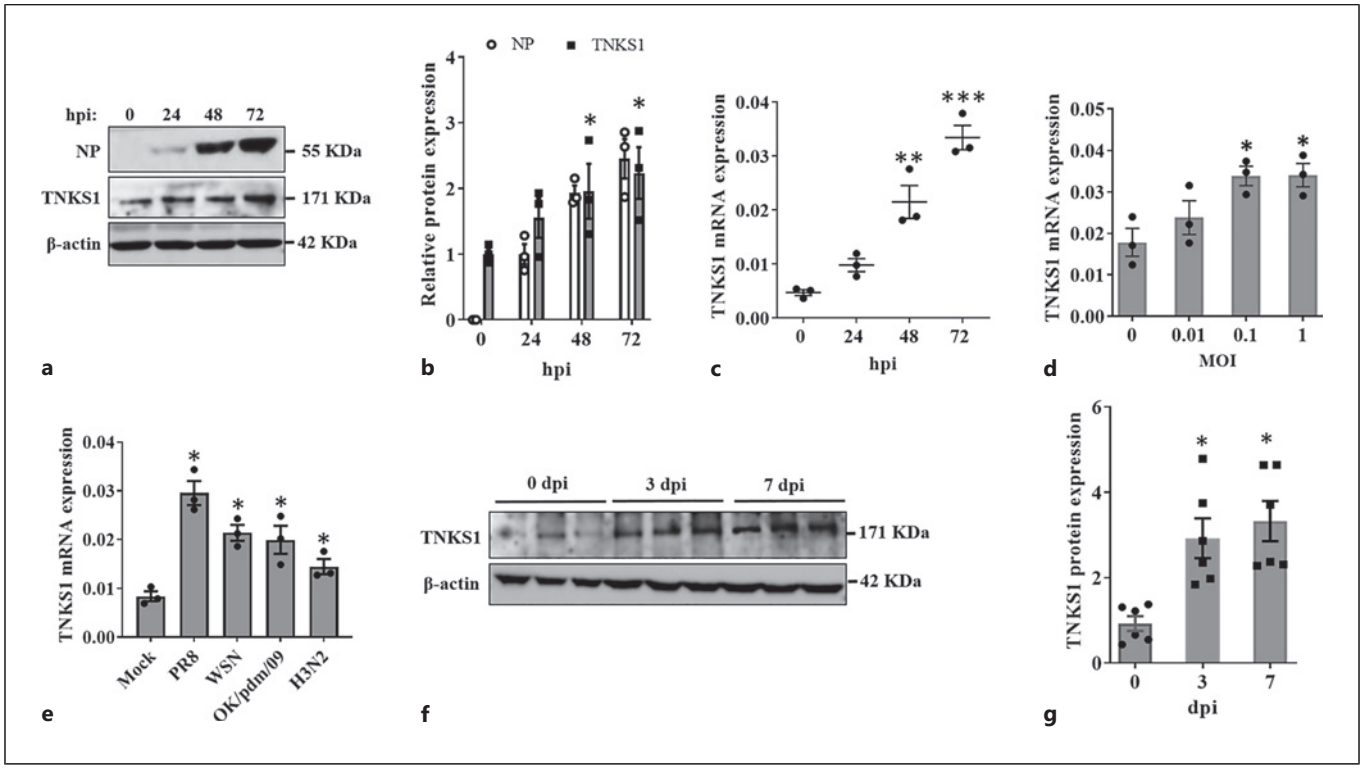

Fig. 1. Influenza virus increases TNKS1 expression. **a**, **b** Human lung epithelial A549 cells were infected with A/PR/8/34 at an MOI of 0.01 for various times (0, 24, 48, and 72 h postinfection or hpi). Viral NP and TNKS1 protein expression levels were determined by Western blot and normalized to β-actin. **a** Representative Western blots. **b** Quantitation of Western blots. The results for TNKS1 and NP were expressed as a ratio to 0 hpi and 24 hpi, respectively. **c**, **d** A549 cells were infected with A/PR/8/34 at an MOI of 0.01 for 0, 24, 48, and 72 h or at different MOI for 24 h. TNKS1 mRNA expression was measured by real-time PCR and normalized to β-actin. **e** A549 cells were infected with A/PR/8/34 (MOI 0.01), A/WSN/33 (MOI 0.001), pdm/OK/09 (MOI 0.01), and H3N2 A/OK/309/06 (MOI 0.001) for 48 h. Relative TNKS1 mRNA expression was measured by real-time PCR and normalized to β-actin. **f**, **g** TNKS1 protein expression levels in the lungs of mice infected with A/PR/8/34 (250 PFU) at 3 and 7 days postinfection (dpi) were measured by Western blot and expressed as a ratio to 0 dpi. The results shown are the mean ± SE. $N = 3$ (cells) or 6 (animals). $^{*}p < 0.05$, $^{**}p < 0.01$ and $^{***}p < 0.001$ versus 0 hpi or 0 dpi, MOI 0 or mock. One-way ANOVA, followed by Dunnett's pairwise comparison.

Because TNKS1 shRNAs reduce IAV replication, we attempted to identify the miRNAs that can target TNKS1 and inhibit IAV infection. TargetScan software (version 6.1) predicts 22 miRNAs with the conserved binding sites on the 3′-UTR of TNKS1. miR-9-1 and miR-140 have two binding sites, while others have one. The same binding site is shared by each pair of miRNAs including miR-34 and miR-449, miR-124 and miR-522, miR-21 and miR-590, and miR-141 and miR-220a. To experimentally validate which miRNAs bind the 3′-UTR of TNKS1, we co-expressed each miRNA expression vector and the TNKS1 3′-UTR luciferase reporter vector into A549 cells. We found that miR-142, miR-30e, miR-190, miR-9-1, miR-522, and miR-140 significantly reduced the reporter activities (Fig. 3a). Although the 3′-UTR reporter assays showed that 6 miRNAs can bind TNKS1, whether these miRNAs have any effects on endogenous TNKS1 protein expression remains to be determined. To test whether these 6 miRNAs have the anti-IAV activities, we co-transfected a miRNA expression vector and an IAV-inducible luciferase reporter vector into A549 cells and infected with A/PR/8/34. We found that only miR-9-1 and miR-30e reduced the luciferase reporter activity (Fig. 3b).

miR-9-1 Inhibits IAV Replication

To further determine the effects of miR-9-1 and miR-30e on IAV infection, we ectopically expressed each of these miRNAs using a GFP-miRNA expression vector and examined viral protein levels in A/PR/8/34-infected HEK293 cells. Transfection efficiency of miRNA plasmids was high and similar among miR-9-1, miR-30e, and

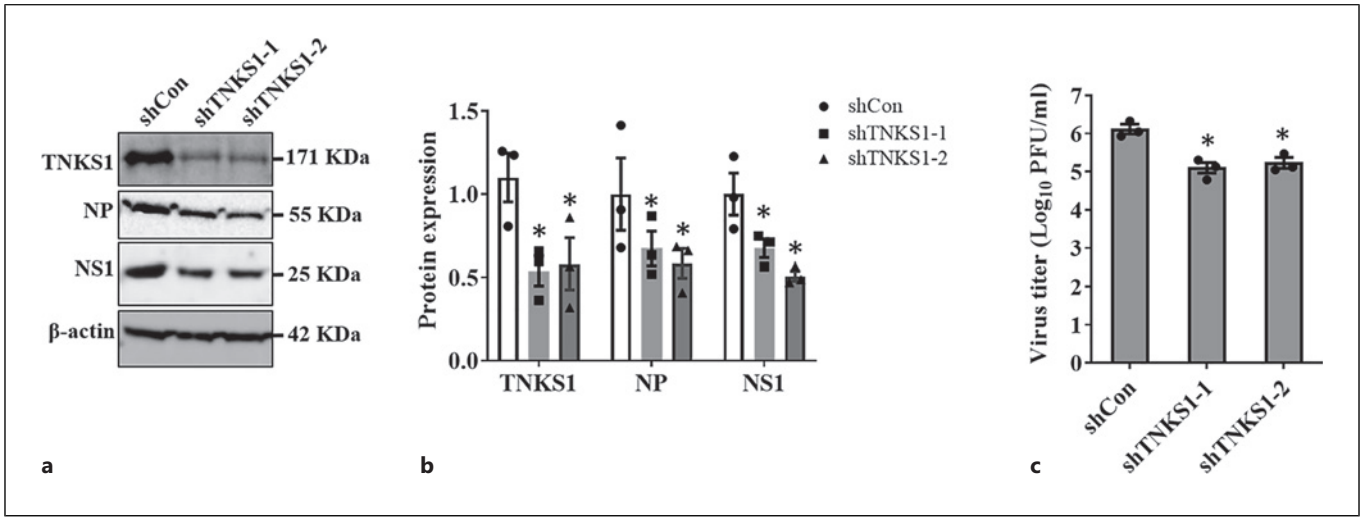

Fig. 2. Knockdown of TNKS1 inhibits IAV replication. HEK293 cells were transfected with a TNKS1 shRNA-1, -2 (shTNKS1-1 and shTNKS1-2) or a control (shCon) plasmid and then infected with A/PR/8/34 at an MOI of 0.01 for 48 h. **a**, **b** The protein levels of TNKS1, viral NP and NS1 were determined by Western blot, normalized to β-actin, and expressed as a ratio to shCon. **a** Representative Western blots. **b** Quantitation of Western blots. **c** Virus titers in the media were measured by the plaque assay. The results shown are the mean ± SE of 3 independent experiments. *$p < 0.05$ versus shCon. One-way ANOVA, followed by Sidak's pairwise comparison.

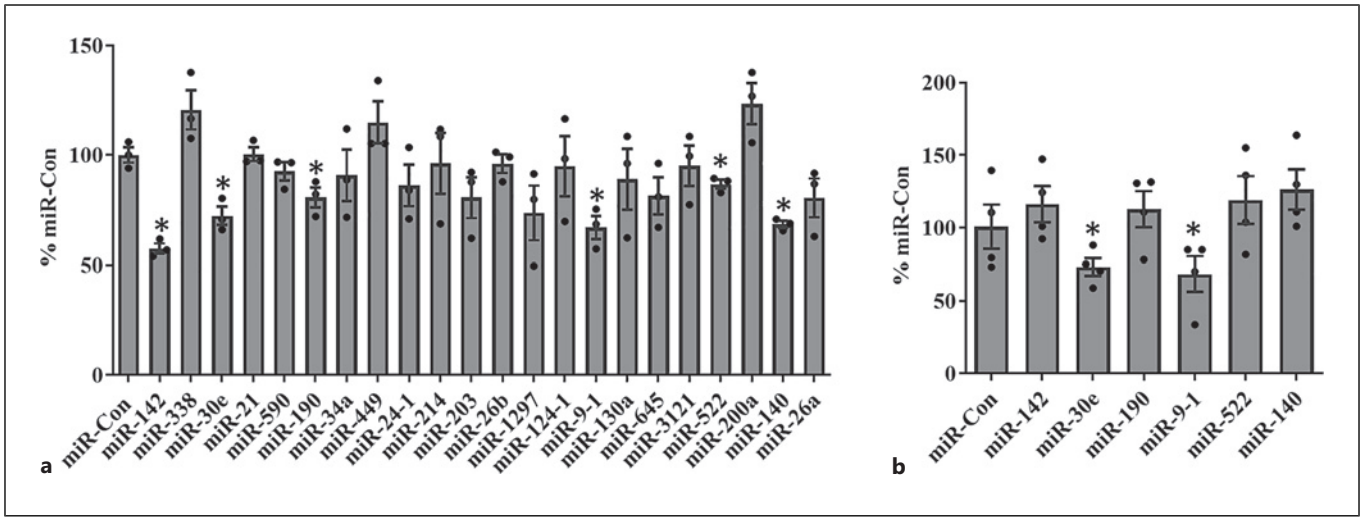

Fig. 3. miRNA screening for targeting TNKS1 and anti-influenza activities. **a** A549 cells were co-transfected with a pmirGLO-firefly-TNKS1-3′-UTR reporter plasmid and a miRNA expression pENTR plasmid or a miRNA control vector (miR-Con) for 24 h, and dual luciferase activities were measured. **b** A549 cells were co-transfected with a miRNA or miR-Con expression pENTR plasmid (100 ng) and the IAV firefly luciferase reporter plasmid vNP-luc/pHH21 (20 ng) and pRL-TK *Renilla* plasmid (5 ng) for 24 h. The cells were then infected with A/PR/8/34 for 48 h, and dual luciferase activities were measured. Relative firefly luciferase activities were normalized to *Renilla* luciferase activities and expressed as a percentage of miR-Con. The results shown are the mean ± SE of 3 or 4 independent experiments. *$p < 0.05$ versus miR-Con, one-way ANOVA, followed by Dunnett's pairwise comparison.

miR-Con as revealed by GFP-positive cells (Fig. 4a; online suppl. Fig. 2). Real-time PCR analysis confirmed the overexpression of miR-9-1 and miR-30e (Fig. 4b). Overexpression of miR-9-1 reduced the protein expression of viral NP and NS1. However, overexpressing miR-30e had no effects on both NP and NS1 protein levels

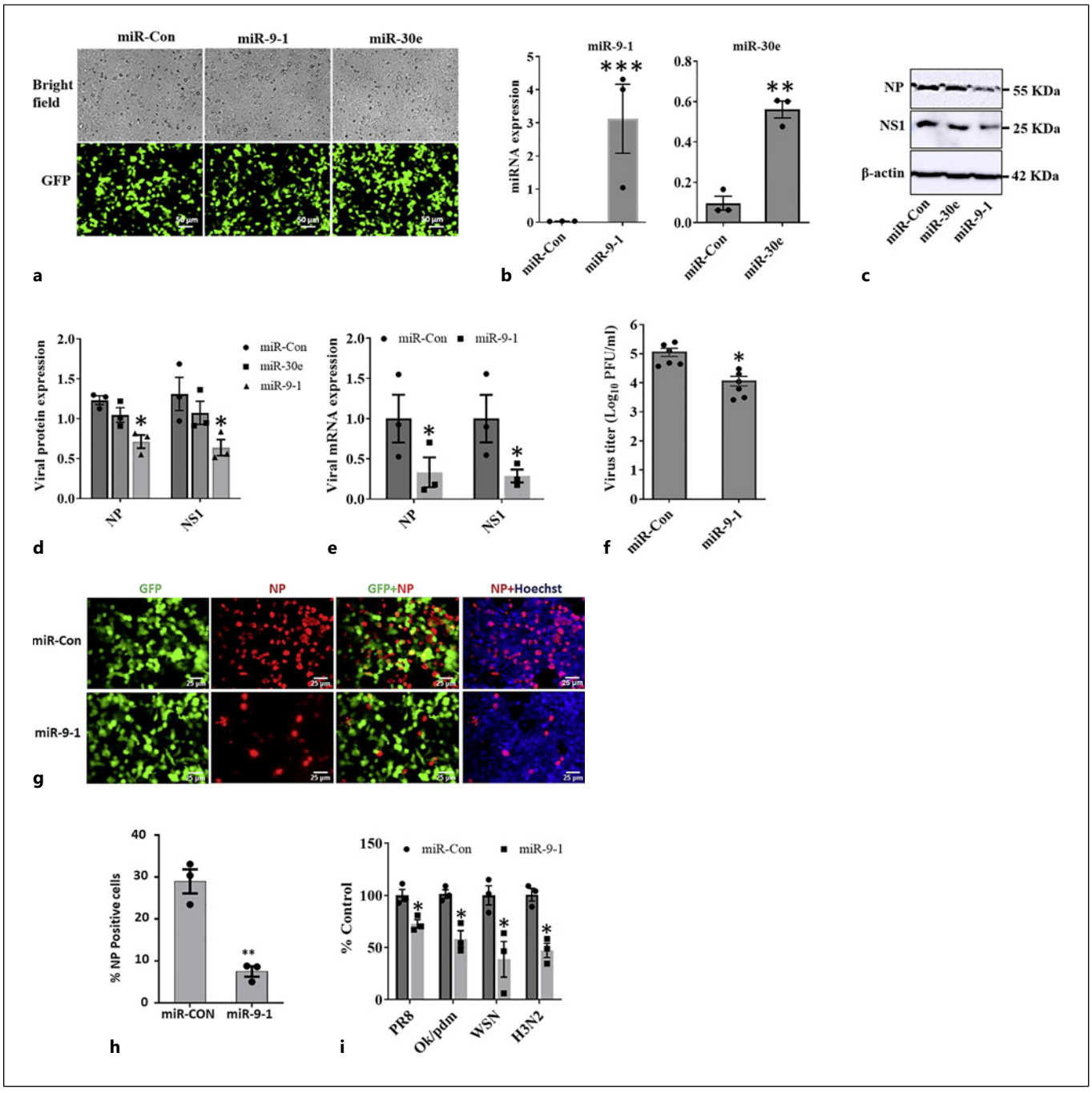

Fig. 4. Inhibition of IAV replication by miR-9-1. HEK293 cells were transfected with a miRNA (miR-9-1 or miR-30e) or miR-Con expression pENTR plasmid for 24 h and then infected with A/PR/8/34 at an MOI of 0.01 for 48 h. **a** Representative GPF images. Scale bars, 50 μm. **b** miRNA expression as determined by real-time PCR and normalized to U6. **c**, **d** The protein expression levels of viral NP and NS1 were determined by Western blot and normalized to β-actin. **c** Representative Western blots. **d** Quantitation of Western blots. **e** The mRNA expression levels of viral NP and NS1 were determined by real-time PCR, normalized to β-actin, and expressed as a ratio to miR-Con. **f** Virus titers in the culture media were determined by plaque assay. **g** GFP images and NP staining. Scale bar: 25 μm. **h** The quantitation of NP-positive cells. **i** HEK293 cells were transfected with a miR-9-1 or miR-Con expression pENTR plasmid (100 ng), the IAV firefly luciferase reporter plasmid vNP-luc/pHH21 (20 ng), and pRL-TK *Renilla* plasmid (5 ng) for 24 h. The cells were then infected with A/PR/8/34 (MOI 0.01), A/WSN/33 (MOI 0.005), pdm/OK/09 (MOI 0.25), and H3N2 A/OK/309/06 (MOI 0.005) for 48 h. Firefly luciferase activities were normalized to *Renilla* luciferase activity and expressed as a percentage of miR-Con. The results shown are the mean ± SE of 3–6 independent experiments. *$p < 0.05$, **$p < 0.01$, and ***$p < 0.001$ versus miR-Con, Student's *t* test for (**b**), (**e**), (**f**), (**h**), and (**i**) and two-way ANOVA followed by Sidak's pairwise comparison for (**d**).

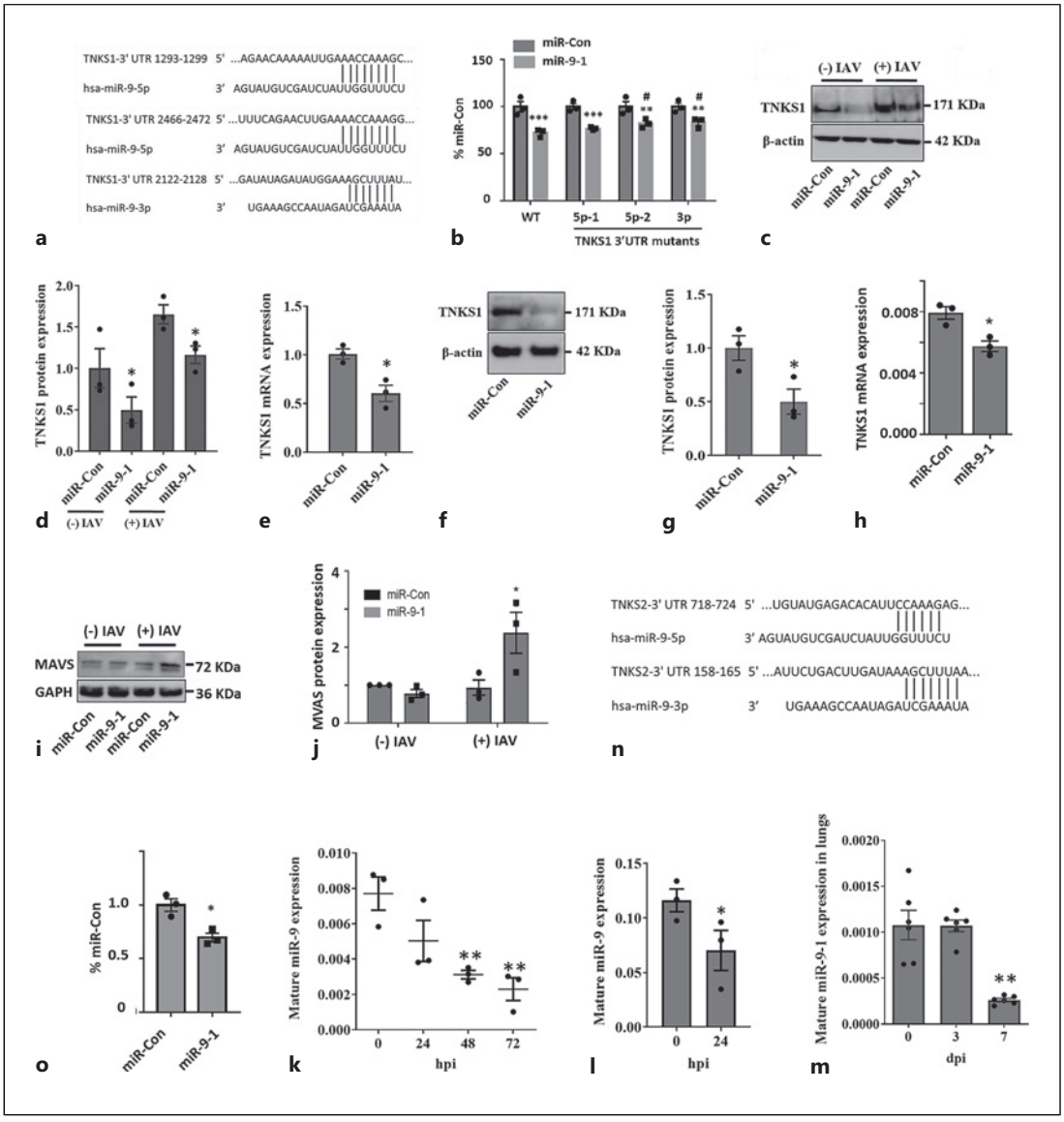

Fig. 5. TNKS1 is a target of miR-9-1. **a** The putative binding sites of miR-9-5p and miR-9-3p in the 3′-UTR of the human TNKS1 gene. **b** A549 cells were co-transfected with a pmirGLO-firefly-TNKS1-3′-UTR wild-type (WT) or miR-9-5p or -3p binding site mutant reporter plasmid and a miRNA expression pENTR plasmid or a miRNA control vector (miR-Con) for 24 h and dual luciferase activities were measured. **c–e** HEK293 cells were transfected with a miR-9-1 or a miR-Con pENTR expression plasmid for 24 h and then infected with and without A/PR/8/34 at an MOI of 0.01 for 48 h. TNKS1 protein levels (**c**, representative blots and **d**, quantitation) were measured by Western blot, normalized to β-actin, and expressed as a ratio to miR-Con without IAV infection. **e** TNKS1 mRNA levels in the cells without IAV infection were measured by real-time PCR, normalized to β-actin and expressed as a ratio to miR-Con. **f–j** A549 cells were transduced with a miR-9-1 or a miR-Con lentivirus for 72 h and then infected with and without A/PR/8/34 at an MOI of 0.01 for 48 h. TNKS1 protein (**f**, representative blots and **g**, quantitation) and MAVS levels (**i**, representative blots and **j**, quantitation) were measured by Western blot, normalized to normalized to β-actin or GAPDH and expressed as a ratio to miR-Con without A/PR/8/34 infection. **h** TNKS1 mRNA levels were measured by real-time PCR and expressed as a ratio of TNKS1/GAPDH. **n** A549 cells were infected with A/PR/8/34 at an MOI of 0.01 for 0, 24, 48, and 72 h. **o** HBTEC cells were infected with A/PR/8/34 at an MOI of 0.1 for 24 h. **k** C57BL/6 mice were infected with A/PR/8/34 (250 PFU) for 3 and 7 days. The endogenous mature miR-9 levels were determined by real-time PCR and normalized to U6. **l** The putative binding sites of miR-9-5p and miR-9-3p in the 3′-UTR of the human TNKS2 gene. **m** A549 cells were co-transfected with a pmirGLO-firefly-TNKS2-3′-UTR reporter plasmid and a miRNA expression pENTR plasmid or a miRNA control vector (miR-Con) for 24 h and dual luciferase activities were measured. The results shown are the mean ± SE. $N = 3$ for cells and $N = 6$ for mice. *$p < 0.05$, **$p < 0.01$, and ***$p < 0.001$ versus miR-Con, 0 hpi or 0 dpi. $^{\#}p < 0.05$ versus WT-miR-9-1. Student's t test for (**d**), (**e**), (**g**), (**h**), (**o**), (**k**), and (**m**). One-way ANOVA, followed by Fisher's LSD for (**b**) or Dunnett's pairwise comparison for (**n**) and (**k**), and two-way ANOVA, followed by Sidak's multiple comparison test (**j**).

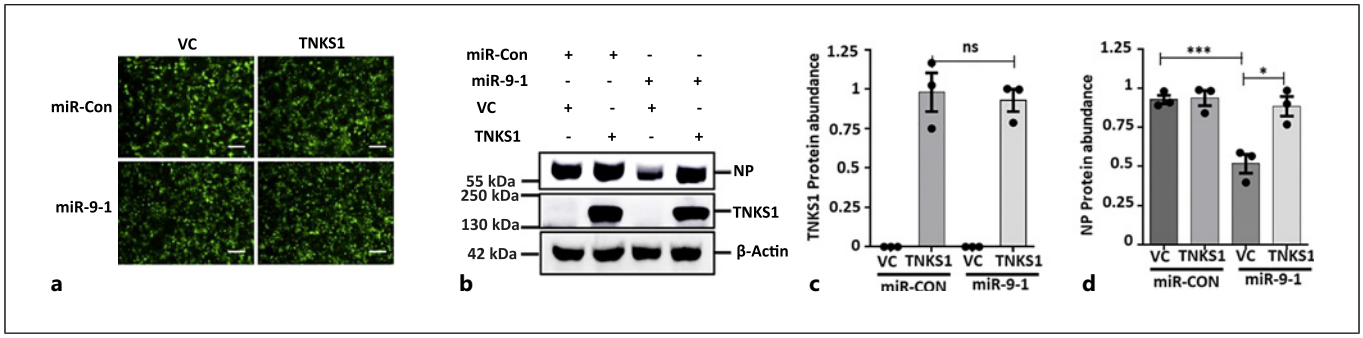

Fig. 6. TNKS1 overexpression rescues the miR-9-1-mediated repression of IAV infection. HEK293T cells were transfected with 625 ng of miR-9-1 or its control, miR-Con pENTR plasmid, and/or 625 ng of PLSJH-TNKS1 or its control, VC. At 24 h post-transfection, cells were infected with a A/PR/8/34 at an MOI of 0.01 for 48 h. **a** The transfection efficiency of miR-9-1 expression plasmid or miR-Con was shown by GFP fluorescence at 24 h post-transfection. Scale bar: 50 μm. **b** TNKS1-Flag and viral protein NP were determined by Western blotting, with β-actin as an internal control. **c**, **d**. The relative amounts of TNKS1-Flag and viral protein NP protein levels were quantitated and normalized to β-actin. The results shown are the mean ± SE of 3 independent experiments. $*p < 0.05$, and $***p < 0.001$ (one-way ANOVA, followed by Tukey's multiple comparisons test). ns, not significant.

(Fig. 4c, d). The reason why miR-30e inhibited the IAV luciferase reporter activity but had no effects on viral protein expression remain to be determined. miR-9-1 also inhibited viral NS1 and NP mRNA expression (Fig. 4e) and virus titer in the medium as determined by plaque assay (Fig. 4f). Immunostaining showed that NP-positive cells were significantly reduced in miR-9-1-overexpressing cells compared to miR-Con-treated cells (Fig. 4g, h). It is noted that in miR-9-1-overexpressed cells, the majority of NP signals (red) did not overlap with GFP signals, confirming the NP reduction in GFP (miR-9-1)-expressing cells.

To determine whether miR-9-1 affects the replication of other strains of IAV, we co-transfected an IAV luciferase reporter vector and miR-9-1 expression vector into HEK293 cells and then infected the cells with H1N1 A/PR/8/34, A/WNS/33, pdm A/OK/3052/09, and H3N2 A/OK/309/06. miR-9-1 attenuated the luciferase activities of the cells infected with all the strains of IAV (Fig. 4g).

Furthermore, we overexpressed miR-9-1 in A549 cells using a lentivirus expressing miR-9-1 (online suppl. Fig. 3A, B). We observed that the overexpression of miR-9-1 suppressed the mRNA and protein levels of viral NS1 in A549 cells and virus titer in the culture media (online suppl. Fig. 3C–F). Additionally, we compared the effects of miR-9-1 on IAV infection between the modes of single and multiple cycles. miR-9-1-overexpressing A549 cells were infected with A/PR/8/34 at an MOI of 1 for 8 h (single cycle) or at an MOI of 0.05 for 48 h (multiple cycles). Cells were immunostained for viral NP. We observed that miR-9-1 significantly reduced NP-positive cells in both single and multiple cycles of infection (online suppl. Fig. 3G, H). Together, these results suggest that anti-influenza activities of miR-9-1 are not dependent on IAV strains and cell types.

miR-9-1 Targeted TNKS1

The TargetScan predicted two conserved miR-9-5p binding sites and one poorly conserved miR-9-3p binding site on the TNKS1 3′-UTR at the positions of 1,293–1,299 (5p-1), 2,466–2,472 (5p-2), and 2,122–2,128 (3p) (Fig. 5a). The results in Figure 3a confirmed the binding of miR-9-1 to the TNKS1 3′-UTR. To determine which binding sites are involved in the binding of miR-9-1, we mutated each binding site and performed the 3′-UTR luciferase reporter assays in A549 cells. The mutations of the second binding site (2,466–2,472) but not the first binding site (1,293–1,299) of miR-9-5p resulted in a partial recovery of luciferase activities compared to the wild-type 3′-UTR (Fig. 5b). Similarly, the mutation of miR-9-3p binding site also restored the luciferase activities partially. The results suggest that both miR-9-5p and miR-9-3p can bind the TNKS1 3′-UTR.

We then determined whether miR-9-1 can suppress the endogenous TNKS1 expression. HEK293 cells were transfected with a miR-9-1 expression vector and infected with A/PR/8/34. miR-9-1 overexpression decreased TNKS1 protein levels by 51 ± 7% and 30 ± 12% in the cells without or with IAV infection, respectively (Fig. 5c, d). Moreover, miR-9-1 overexpression also decreased TNKS1 mRNA expression in HEK293 cells (Fig. 5e). A similar reduction in TNKS1 protein and mRNA levels was also

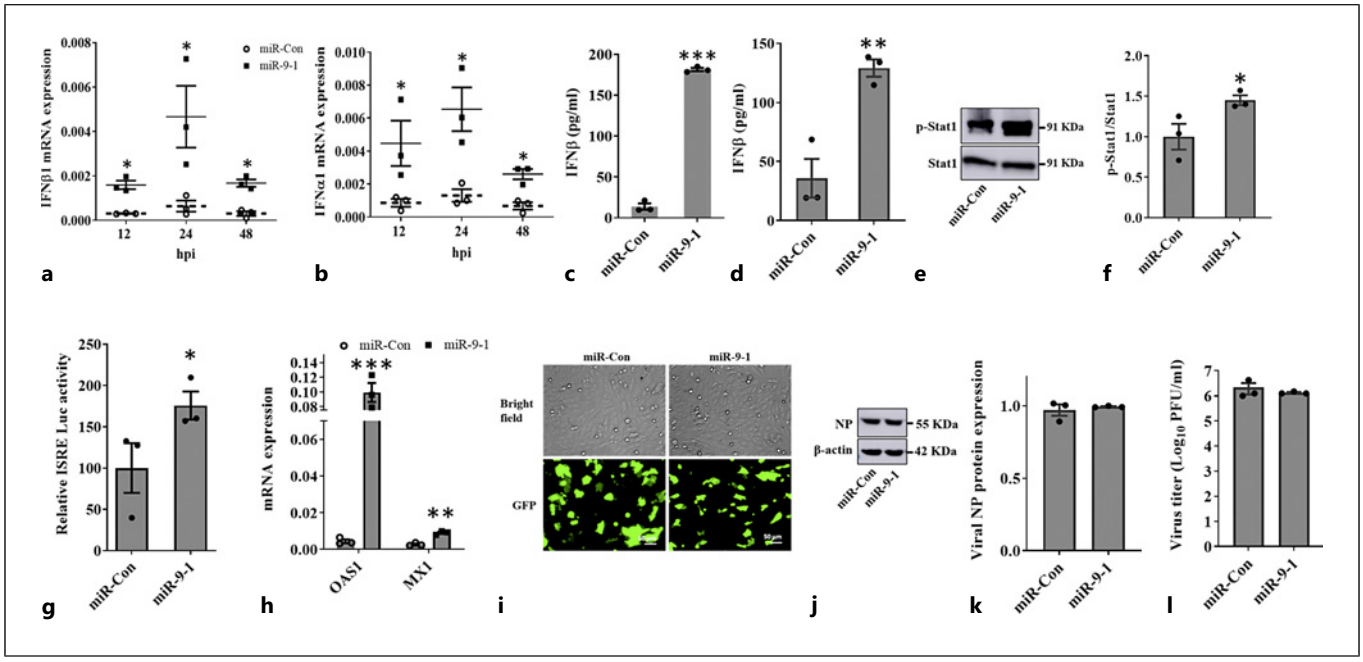

Fig. 7. miR-9-1 activates an antiviral state. **a**, **b** HEK293 were transfected with a miR-9-1 or a miR-Con pENTR expression plasmid for 24 h and infected with A/PR/8/34 at an MOI of 0.01 for 12, 24, and 48 h. The mRNA expression levels of IFNβ1 and IFNα1 were determined by real-time PCR and normalized to β-actin. **c**, **d** IFNβ production in the media of HEK293 and A549 cells infected with A/PR/8/34 at an MOI of 0.01 for 24 h were measured by ELISA. **e**, **f** HEK293 cells were transfected with a miR-9-1 or a miR-Con pENTR expression plasmid for 24 h and then infected with A/PR/8/34 at an MOI of 0.01 for 48 h. The protein expression levels of p-Stat1 and Stat1 were determined by Western blot and expressed as a ratio of p-Stat1 to Stat1 and then a ratio to miR-Con. **g** HEK293 cells were co-transfected with a miR-9-1 or a miR-con expression pENTR plasmid, and an ISRE-Luc reporter vector for 24 h and then infected with A/PR/8/34 at an MOI of 0.01 for 48 h. Dual luciferase activities were measured and the firefly activities were normalized to *Renilla* luciferase activities. The results were expressed as a percentage of miR-Con. **h** HEK293 cells were infected with A/PR/8/34 at an MOI of 0.01 for 48 h. The mRNA expression levels of OAS1 and MX1 were measured by real-time PCR and normalized to β-actin. **i–l** Vero cells were transfected with a miR-9-1 or a miR-Con expression pENTR plasmid for 24 h and then infected with A/PR/8/34 at an MOI of 0.01 for 48 h. GFP images are shown in (**i**). Viral NP protein levels (**j**, representative blots and **k**, quantitation) and virus titers (**l**) were measured by Western blot and plaque assay, respectively. The results shown are the mean ± SE of 3 independent experiments. $*p < 0.05$, $**p < 0.01$, and $***p < 0.001$ versus miR-Con. Two-way ANOVA, followed by Tukey's pairwise comparison for (**a**) and (**b**); Student's *t* test for (**c**), (**d**), (**f**), (**g**), (**h**), (**k**), and (**l**).

observed in miR-9-1-overexpressed and uninfected A549 cells (Fig. 5f–h). These results indicate that miR-9-1 reduces TNKS1 level via mRNA degradation.

TNKS1 and TNKS2 have been shown to enhance MAVS degradation [51]. As miR-9-1 reduces the TNKS1 protein level, we expect that miR-9-1 increases the MAVS protein level. Indeed, overexpression of miR-9-1 increases the MAVS protein levels in the IAV-infected cells (Fig. 5i, j).

The results from Figure 1 showed that IAV increased TNKS1 expression. Here, we observed a gradual decrease in endogenous mature miR-9 in A549 cells infected with A/PR/8/34 in a time-dependent manner (Fig. 5k). This reduction was also seen in IAV-infected primary human lung epithelial cells, HBTEC, and in the lungs of IAV-C57BL/6 mice (Fig. 5l, m). The inverse correlation of TNKS1 and mature miR-9 expression further supports that TNKS1 is an endogenous target of miR-9-1 in lung epithelial cells.

The TargetScan also predicted one conserved miR-9-5p and one poorly conserved miR-9-3p bindings at 718–724 and 158–165 of the TNKS2 3′-UTR (Fig. 5n). 3′-UTR assay revealed that miR-9-1 could bind TNKS2 (Fig. 5o).

miR-9-1 Inhibits IAV Infection by Targeting TNKS1

To determine whether TNKS1 is involved in miR-9-1-mediated reduction in IAV infection, we performed a rescue experiment, in which TNKS1 and miR-9-1 were co-expressed in cells. HEK293T were transfected with or without a TNKS1 plus Flag tag expression plasmid and/or

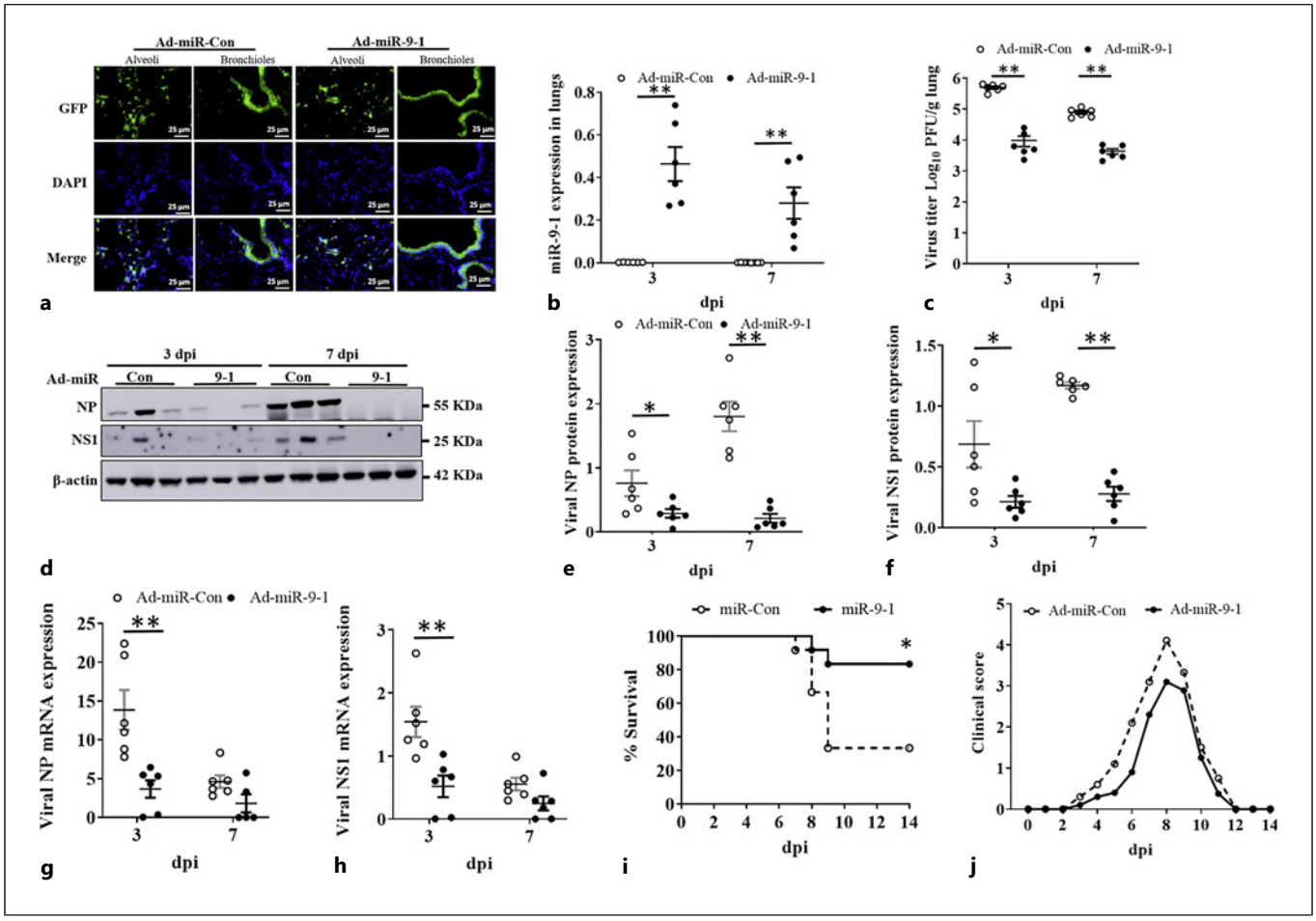

Fig. 8. Adenovirus expressing miR-9-1 suppresses IAV infection in vivo and increases survival of mice against IAV infection. An adenovirus expressing miR-9-1 (Ad-miR-9-1) or miR-Con (Ad-miR-Con) was delivered intratracheally into the lungs of male and female mice. Two days after, the mice were infected intranasally with A/PR/8/34 (160 PFU/mouse). The samples were collected at 3 and 7 days postinfection (dpi). **a** GFP expression in the lungs was determined by immunofluorescent staining in paraformaldehyde-fixed lung tissue sections at 3 dpi. Scale bar, 25 μm. **b** miR-9-1 levels in the lung tissues were measured by real-time PCR and normalized to U6 snRNA. **c** The virus titers were determined by plaque assay. **d**–**f** Viral NP and NS1 protein levels in the lung tissues were determined by Western blot and normalized to β-actin. **g**, **h** The mRNA levels of viral NP and NS1 were determined by real-time PCR and normalized to β-actin. For (**b, c**), (**e–h**), the results of 6 animals (3 males and 3 females) per group are displayed as the mean ± SE. *$p < 0.05$, **$p < 0.01$, two-way ANOVA, followed by Sidak's multiple comparisons. **i, j** Two days after Ad-miR-9-1 or Ad-miR-con delivery, mice (female, $N = 12$ per group) were intranasally infected with A/PR/8/34 (×1 MLD50). Survival curve and clinical scores are shown in (**i**) and (**j**). *$p < 0.05$ versus Ad-miR-Con, Mantel-Cox test with Bonferroni-corrected threshold.

a miR-9-1 plus GFP tag expression vector, followed by infection with A/PR/8/34. The expression of miR-9-1 and TNKS1 were confirmed by GFP images (Fig. 6a) and Western blotting with anti-Flag antibodies (Fig. 6b, c). As expected, overexpression of miR-9-1 without TNKS1 transfection reduced viral NP levels. Co-transfection of miR-9-1 and TNKS1 restored the NP levels (Fig. 6b, d), suggesting that the effect of miR-9-1 on IAV infection is through TNKS1.

miR-9-1 Induces Type I IFN Responses

Host cells elicit robust IFN responses that are central to defend against viral infections. We thus examined the effects of miR-9-1 on type I IFN responses. We first investigated whether miR-9-1 induces type I IFN expression and production. miR-9-1-overexpressing HEK293 cells were infected with A/PR/8/34 for different times. miR-9-1 increased the mRNA expression of IFNβ1 and IFNα1 with a peak at 24 hpi (Fig. 7a, b). IFNβ protein

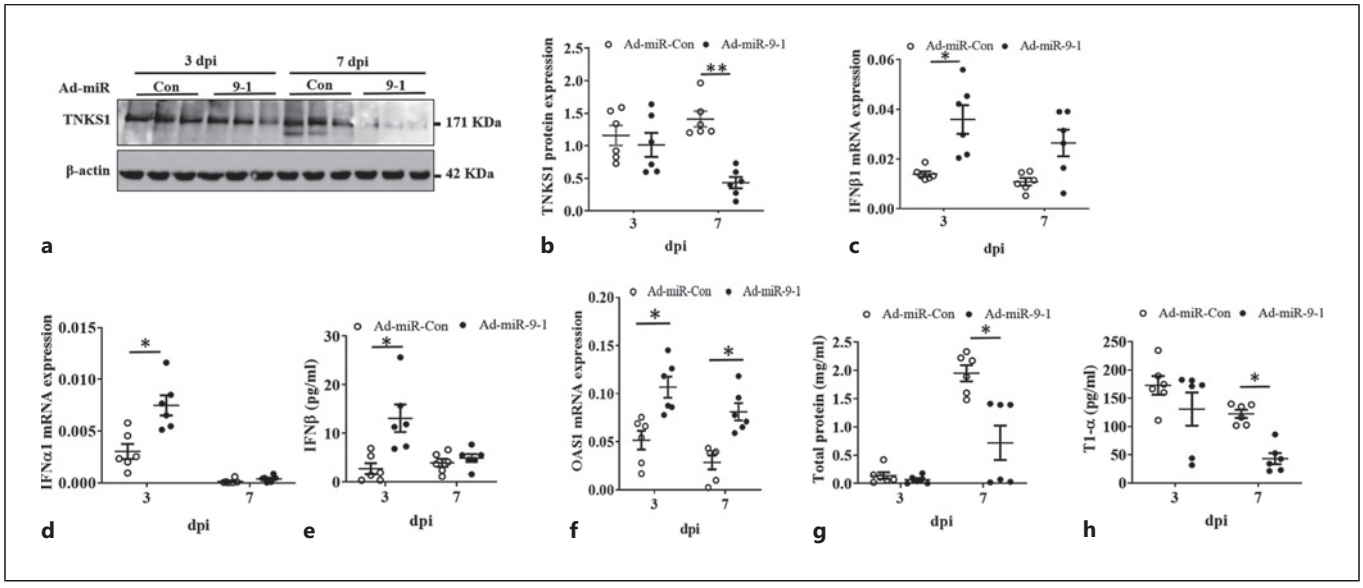

Fig. 9. miR-9-1 activates the antiviral state and reduces lung injury in mice. An adenovirus expressing miR-9-1 (Ad-miR-9-1) or miR-Con (Ad-miR-Con) was delivered intratracheally into the lungs of male and female mice. Two days after, the mice were infected intranasally with A/PR/8/34 (160 PFU/mouse). The samples were collected at 3 and 7 days postinfection (dpi). **a**, **b** TNKS1 protein levels were measured by Western blot and normalized to β-actin. **c**, **d** The mRNA levels of IFNβ1 and IFNα1 were measured by real-time PCR and normalized to β-actin. **e** IFNβ production in BALF was measured by ELISA. **f** OAS1 mRNA levels were measured by real-time PCR and normalized to β-actin. **g** Total proteins in BALF were measured by D_C protein assay. **h** T1-α protein amounts in BALF were measured by ELISA. The results shown are the mean ± SE. $N = 6$ (3 males and 3 females). *$p < 0.05$ and **$p < 0.01$, two-way ANOVA, followed by Sidak's multiple comparisons.

production in the medium at 24 hpi was increased 13 folds by miR-9-1 (Fig. 7c). miR-9-1-mediated increase of IFNβ protein in the medium was also observed in A/PR/8/34-infected A549 cells (Fig. 7d).

Type I IFNs activate the Stat signaling through the phosphorylation of the transcription factor Stat1, the nuclear translocation of the phosphorylated Stat1, and the binding of the Stat1 to ISREs of IFN-stimulated genes (ISGs), leading to an increase in the expression of ISGs. We next examined whether miR-9-1 activates the Stat signaling by monitoring the phosphorylation of Stat1, ISRE luciferase reporter activity, and ISG expression. miR-9-1 enhanced the phosphorylation of Stat1 in the A/PR/8/34-infected HEK293 cells (Fig. 7e, f). miR-9-1 also increased the ISRE luciferase reporter activities (Fig. 7g). Furthermore, miR-9-1 increased the mRNA levels of two ISGs, OAS1 and MX1 (Fig. 7h).

To further confirm that the antiviral effects of miR-9-1 involve the type I IFN signaling, we examined whether miR-9-1 had any effects on IAV infection in Vero cells that are unable to produce type I IFNs [52]. Vero cells were transfected with miR-9-1 or miR-Con plasmid. GFP images revealed a similar transfection efficiency (Fig. 7i; online suppl. Fig. 4). The miR-9-1-overexpressed Vero cells were then infected with A/PR/8/34, and viral NP protein expression in cells and viral titers in culture media were determined. miR-9-1 had no effects on NP levels in Vero cells and viral titers in media (Fig. 7j–l). Our results suggest that miR-9-1 activates type I IFN responses to restrict IAV infection.

miR-9-1 Has Antiviral Activities in Mice

In vivo delivery of miRNAs can be achieved by using virus-based vector systems such as lentiviruses, retroviruses, adenoviruses, or adeno-associated viruses [53]. Each system has its pros and cons. An adenoviral vector has a high transduction efficiency, but it cannot be integrated to the host genome. It is often used for a short-term expression [54]. We utilized an adenoviral system to deliver miR-9-1 to mouse lungs and investigated its effects on IAV infection in vivo.

Mice received an adenovirus expressing miR-9-1 (Ad-miR-9-1) or its control (Ad-miR-Con) intratracheally. Two days later, the mice were then infected with a sublethal dose of A/PR/8/34. Lung tissue samples were collected at 3 and 7 dpi. Using immunofluorescent staining, we first determined the localization of GFP, a tag protein included in the adenoviral vector, to confirm the

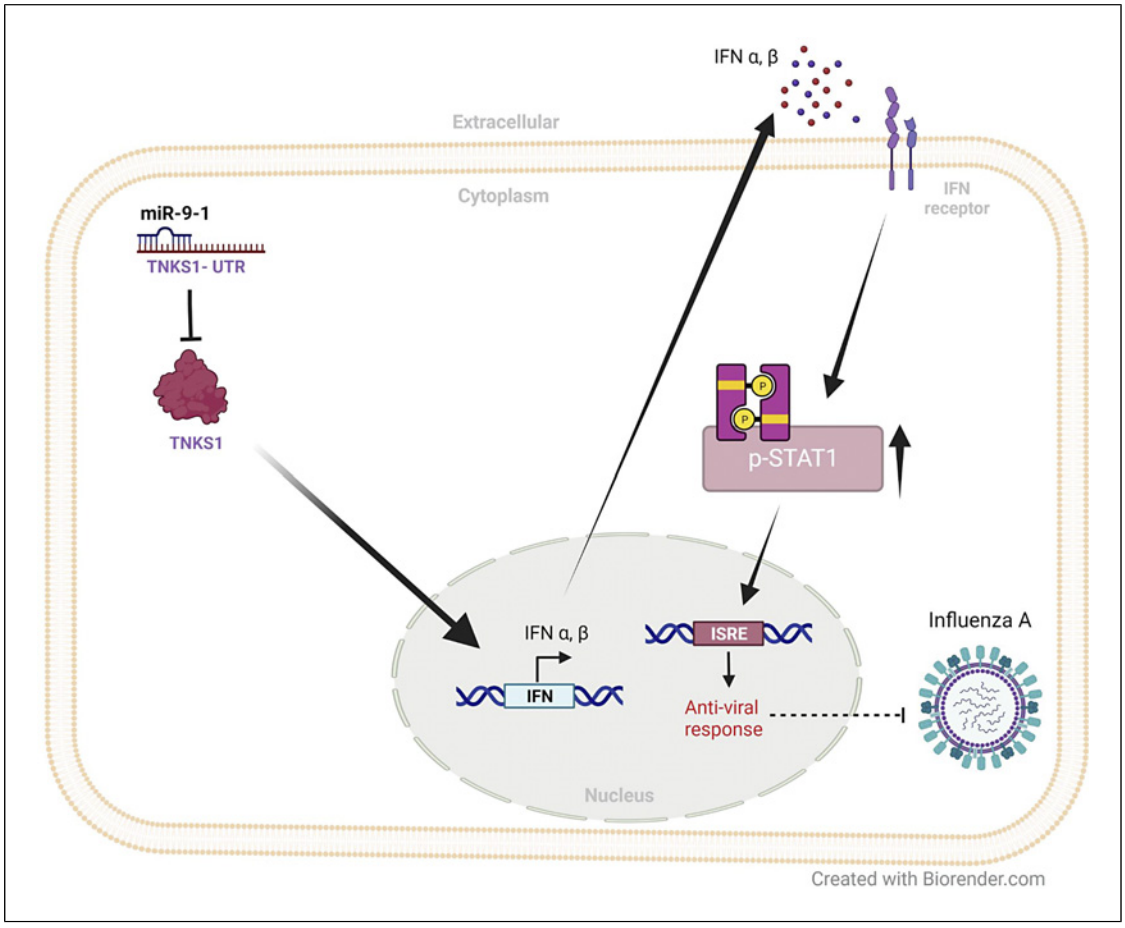

Fig. 10. A schematic overview of the current study.

delivery of miR-9-1 into the lungs of mice. We observed GFP expression in both small airway and alveolar regions (Fig. 8a). Compared to the mice that received Ad-miR-Con, miR-9-1 expression in the lungs of Ad-miR-9-1-treated mice was increased 175- and 161-folds at 3 and 7 dpi, respectively (Fig. 8b). Ad-miR-9-1 decreased viral titers in the lungs at both time points (Fig. 8c). Moreover, Ad-miR-9-1 also reduced the protein and mRNA expression of viral genes, NP and NS1 (Fig. 8d–f).

We further performed a survival study using a 50% lethal dose of influenza virus A/PR/8/34. Ad-miR-9-1 significantly increased the survival of mice compared to Ad-miR-Con (Fig. 8h). Clinical scores in the Ad-miR-9-1 group were lower than these in the Ad-miR-Con group (Fig. 8i). The results indicate that miR-9-1 protects mice against influenza virus infection.

To determine the antiviral mechanisms of miR-9-1 in vivo, we first determined the TNKS1 protein expression. Ad-miR-9-1 significantly reduced TNKS1 protein expression in the lungs at 7 dpi (Fig. 9a, b). miR-9-1 overexpression enhanced type I IFN signaling in vitro (Fig. 7). We thus examined the type I IFN and ISG expression in the lungs of Ad-miR-9-1-treated mice. Ad-miR-9-1 increased the mRNA expression of IFNβ1 and IFNα1 in the lung tissue and IFNβ protein levels in the BALF at 3 dpi (Fig. 9c–e). Ad-miR-9-1 also augmented the mRNA expression of the ISG, OAS1 (Fig. 9f). In miR-9-1-overexpressing lungs, TNKS1 protein level showed a decrease trend at 3 dpi but did not reach significant level while IFNα1, IFNβ1, and ISG exhibited a significant increase at 3 dpi. One possible explanation is that the whole lung tissue was used for Western blot, and the changes in TNKS1 level in whole lung tissues do not reflect the cell types for IAV infection and/or miR-9-1 overexpression. Another possibility is that miR-9-1 could activate type I IFN signaling via additional mechanisms besides targeting TNKS1.

Finally, we examined the IAV-mediated lung injury of Ad-miR-9-1-treated mice by measuring total proteins and T1-α, a cellular marker for alveolar epithelial type I cells. Ad-miR-9-1 significantly reduced the total proteins and T1-α released into the BALF (Fig. 9g, h), suggesting that miR-9-1 reduces lung injury.

Discussion

All currently approved anti-influenza drugs belong to direct-acting antivirals that target viral proteins and hinder viral replication. Even though direct-acting antivirals have a lower tendency for undesirable side effects compared to the indirect-acting antivirals, they can rapidly develop drug resistance due to the error-prone viral RNA polymerases [55]. Several drugs targeting host factors to treat influenza overcome the drug resistance problem and are in various stages of development including siRNAs [56]. Host miRNAs play pivotal roles in several cellular processes including defense against viral infections. In this study, we observed that (1) IAV induced endogenous TNKS1 expression in vitro and in vivo, (2) TNKS1 knockdown attenuated IAV replication, (3) miR-9-1 inhibited IAV infection in cell culture and mouse model by activating antiviral innate immunity possibly via targeting TNKS1/STAT1, and (4) miR-9-1 overexpression in the mouse lungs increased survival and reduced IAV-induced lung injury. Based on these results, we proposed a model in which miR-9-1 reduces TNKS1 expression, in turn induces the expression of type I IFN, activates STAT1, induces ISGs, and finally represses IAV replication (Fig. 10).

Posttranslational modifications such as phosphorylation and ubiquitination of viral proteins or host cellular proteins are a common phenomenon in the host-virus interactions. However, the role of ADP-ribosylation in the host-virus conflict is less studied. Many PARPs were found to be evolved with host-virus conflicts and play an important role in host immunity [57]. Several viral families evolve to encode for macrodomains that interfere with ADP-ribosylation and are critical for host immune evasion [58]. In the host, PARP13/ZAPL has broad antiviral activities against several viral infections including IAV [59]. PARP1 is required for IAV RNA polymerase activity [60]. PARP1 also facilitates IAV-induced degradation of host type I IFN receptor and promotes immune evasion [12]. In this study, we added the additional member of the PARP family, TNKS1 (PARP5a) as a proviral factor for IAV infection.

We observed that TNKS1 expression was induced during influenza virus infection. This is consistent with a previous study that both TNKS1 and 2 were induced by HCMV [21]. However, HSV suppresses TNKS1 expression and has no effects on TNKS2 expression [22]. Our present study also demonstrated that knockdown of TNKS1 reduced IAV protein levels and titers, suggesting the proviral role of TNKS1. This is consistent with two previous studies: TNKS knockdown or inhibition of its activity reduces HCMV replication [21]. TNKS1 facilitates HSV infection via its nuclear translocation in an ICP0- and ERK-dependent manner [22]. However, our results contrast with another study, in which TNKS2 inhibits Epstein-Barr virus replication by interacting with Epstein-Barr virus nuclear antigen 1 [20]. Collectively, our current observations and previous findings suggest that the changes in TNKS expression in response to viral infection and the action of TNKS on virus infection depend on the types of viruses.

Our current studies demonstrate that TNKS1 is a target of miR-9-1, which is supported by (1) there are predicted miR-9-1 binding sites on TNKS1 3′-UTR, (2) 3′-UTR luciferase reporter assays showed the binding of miR-9-1 with TNKS1, (3) overexpression of miR-9-1 in HEK293 and A549 cells reduced TNKS1 protein levels, and (4) IAV increased TNKS1, but reduced miR-9-1 expression in vitro and vivo. However, we cannot rule out the possibility that miR-9-1 also exerts its anti-influenza virus activities via other targets. For example, miR-9-1 has been reported to target NFκB p50 in human monocytes, neutrophils, and ovarian cancer cells [39, 61], and repression of NKκB has been shown to increase IFN responses [62].

In consistent with IAV-induced increases in TNKS1 expression, we found that endogenous miR-9-1 levels were downregulated in IAV-infected cells and mouse lungs in a time-dependent manner. In one previous study, miR-9 was found to be increased in the influenza virus-infected A549 cells with a peak at 12 hpi [41]. The reason for the disagreement is unclear. miR-9 was also upregulated in the cortex of Zika virus-infected mice [40] and in HIV transactivating regulatory protein (Tat)-stimulated astrocytes [63]. High levels of miR-9 were associated with human papillomavirus-induced cervical cancers [64].

In the present study, we demonstrated that miR-9-1 inhibited the replication of different IAV strains (H1N1 A/PR/8/34, pdm/OK/2009, A/WSN/33, and H3N2 A/OK/309/06) in two types of cells (A549 cells and HEK293 cells) using multiple assays including viral mRNA and protein expression in host cells and viral titers in culture media as well as an IAV reporter assay. Furthermore, we found that overexpression of miR-9-1 in the mouse lungs reduced viral load and increased survival. These in vitro and in vivo data support an antiviral role of

miR-9-1 in influenza virus infection. Contradictory to our finding, Dong et al. [41] has shown that the transfection of miR-9 synthetic mimics promotes IAV replication in A549 cells. One of the possible reasons for the difference is the method for overexpression of miR-9-1. We used a plasmid to express a miR-9-1 precursor, which undergoes the processing in cells to become mature miR-9-1 and avoids an overwhelming load of miRNAs into cells. In contrast, Dong et al. [41] used chemically synthesized miR-9 mimic. It is unclear that what level of miR-9 mimic expression was achieved in their studies.

Our data support that miR-9-1 increases IFN responses during influenza infection. This conclusion was supported by the following in vitro and in vivo observations: (1) miR-9-1 induced mRNA and protein expression of type I IFNs (IFNα and IFNβ) during IAV infection, (2) miR-9-1 increased the phosphorylation of Stat1, (3) miR-9-1 increased transcriptional activity of Stat1 as shown by an ISRE reporter assay, (4) miR-9-1 enhanced the expression of ISGs, and (5) miR-9-1 had no effects on IAV replication in the IFN-deficient Vero cells. A recent study shows that TNKS1 inhibits type I IFN response using knockout cells [51]. As we found that miR-9-1 targeted TNKS1, it is likely that the reduction in TNKS1 expression caused by miR-9-1 results in the enhanced IFN response. Based on published data, two mechanisms by which the repression of TNKS1 induces type I IFN response can be speculated: (1) increasing MAVS. TNKS1 and TNKS2 have been reported to inhibit type I IFN response by polyADP-ribosylation MAVS and thus inducing its degradation [51]. Our current study supports this mechanism as we showed that miR-9-1 reduced TNKS1 protein levels but increased MAVS protein levels. (2) Increasing Axin1 level. The inhibition of TNKS is known to prevent Axin1 degradation [65]. We have recently shown that Axin1 enhances IAV-induced IFN response [66]. Thus, miR-9-1-mediated reduction in TNKS1 expression could increase Axin1 level and IFN response.

In summary, we identified miR-9-1 as a miRNA that targets TNKS1 and showed that miR-9-1 inhibited IAV replication in vitro and in vivo and enhanced type I IFN signaling. The findings of our studies may contribute to the knowledge of developing potential miRNA-based anti-influenza therapeutics.

Acknowledgments

We thank Dr. Gillian Air (University of Oklahoma Health Sciences Center) for providing the IAV viral strains (A/Oklahoma/3052/09 H1N1, H3N2 A/Oklahoma/309/2006, and A/WSN/1933 H1N1) and Drs. Amit Bhardwaji and Susan Smith (New York University School of Medicine) for providing TNKS1 overexpression vector (pLSJH-TNKS1).

Statement of Ethics

All animal experimental protocols were reviewed and approved by the Institutional Animal Care and Use Committee (IACUC) of Oklahoma State University (approval number: VM-15-38).

Conflict of Interest Statement

The authors have no conflicts of interest.

Funding Sources

This work was supported by the National Institutes of Health grants AI152004, AI121591, HL135152, and GM103648, the Oklahoma Center for Adult Stem Cell Research – A Program of Tobacco Settlement Endowment Trust (TSET), the Oklahoma Center for the Advancement of Science and Technology (HR-20-050), and the Lundberg-Kienlen Endowment Fund (to L.L.).

Author Contributions

Gayan Bamunuarachchi performed experiments, analyzed data, and wrote the manuscript. Kishore Vaddadi, Xiaoyun Yang, Quanjin Dang, Zhengyu Zhu, Sankha Hewawasam, Chaoqun Huang, Yurong Liang, and Yujie Guo performed experiments and analyzed data. Lin Liu designed the concept of the manuscript, provided resources, analyzed data, and wrote the manuscript.

Data Availability Statement

All data generated or analyzed during this study are included in this article and its supplementary material files. Further inquiries can be directed to the corresponding author.

References

1 Center of Disease Control. Disease burden of influenza; 2020. Available from: https://www.cdc.gov/flu/about/burden/index.html.

2 Taubenberger JK, Morens DM. 1918 Influenza: the mother of all pandemics. Emerg Infect Dis. 2006;12(1):15–22.

3 Krammer F, Smith GJD, Fouchier RAM, Peiris M, Kedzierska K, Doherty PC, et al. Influenza. Nat Rev Dis Primers. 2018;4(1):3.

4 Bouvier NM, Palese P. The biology of influenza viruses. Vaccine. 2008;26(Suppl 4): D49–53.
5 Principi N, Camilloni B, Alunno A, Polinori I, Argentiero A, Esposito S. Drugs for influenza treatment: is there significant news? Front Med. 2019;6:109.
6 Yip TF, Selim ASM, Lian I, Lee SMY. Advancements in host-based interventions for influenza treatment. Front Immunol. 2018;9: 1547.
7 Morales J, Li L, Fattah FJ, Dong Y, Bey EA, Patel M, et al. Review of poly (ADP-ribose) polymerase (PARP) mechanisms of action and rationale for targeting in cancer and other diseases. Crit Rev Eukaryot Gene Expr. 2014;24(1):15–28.
8 Kuny CV, Sullivan CS. Virus–host interactions and the ARTD/PARP family of enzymes. PLoS Pathog. 2016;12(3):e1005453.
9 Fehr AR, Singh SA, Kerr CM, Mukai S, Higashi H, Aikawa M. The impact of PARPs and ADP-ribosylation on inflammation and host-pathogen interactions. Genes Dev. 2020; 34(5–6):341–59.
10 Zhu H, Tang YD, Zhan G, Su C, Zheng C. The critical role of PARPs in regulating innate immune responses. Front Immunol. 2021;12:712556.
11 Zhu H, Zheng C. When PARPs meet antiviral innate immunity. Trends Microbiol. 2021; 29(9):776–8.
12 Xia C, Wolf JJ, Sun C, Xu M, Studstill CJ, Chen J, et al. PARP1 enhances influenza A virus propagation by facilitating degradation of host type I interferon receptor. J Virol. 2020;94(7):e01572-19–.
13 Hayakawa S, Shiratori S, Yamato H, Kameyama T, Kitatsuji C, Kashigi F, et al. ZAPS is a potent stimulator of signaling mediated by the RNA helicase RIG-I during antiviral responses. Nat Immunol. 2011;12(1):37–44.
14 Zhang Y, Mao D, Roswit WT, Jin X, Patel AC, Patel DA, et al. PARP9-DTX3L ubiquitin ligase targets host histone H2BJ and viral 3C protease to enhance interferon signaling and control viral infection. Nat Immunol. 2015; 16(12):1215–27.
15 Atasheva S, Frolova EI, Frolov I. Interferon-stimulated poly(ADP-ribose) polymerases are potent inhibitors of cellular translation and virus replication. J Virol. 2014;88(4): 2116–30.
16 Li L, Zhao H, Liu P, Li C, Quanquin N, Ji X, et al. PARP12 suppresses Zika virus infection through PARP-dependent degradation of NS1 and NS3 viral proteins. Sci Signal. 2018; 11(535):eaas9332.
17 Ficarelli M, Antzin-Anduetza I, Hugh-White R, Firth AE, Sertkaya H, Wilson H, et al. CpG dinucleotides inhibit HIV-1 replication through Zinc finger Antiviral Protein (ZAP)-dependent and -independent mechanisms. J Virol. 2020;94(6):e01337–19.
18 Riffell JL, Lord CJ, Ashworth A. Tankyrase-targeted therapeutics: expanding opportunities in the PARP family. Nat Rev Drug Discov. 2012;11(12):923–36.
19 Angelova M, Zwezdaryk K, Ferris M, Shan B, Morris CA, Sullivan DE. Human cytomegalovirus infection dysregulates the canonical Wnt/β-catenin signaling pathway. PLoS Pathog. 2012;8(10):e1002959.
20 Deng Z, Atanasiu C, Zhao K, Marmorstein R, Sbodio JI, Chi NW, et al. Inhibition of Epstein-Barr virus OriP function by tankyrase, a telomere-associated poly-ADP ribose polymerase that binds and modifies EBNA1. J Virol. 2005;79(8):4640–50.
21 Roy S, Liu F, Arav-Boger R. Human cytomegalovirus inhibits the PARsylation activity of tankyrase: a potential strategy for suppression of the Wnt pathway. Viruses. 2015; 8(1):8.
22 Li Z, Yamauchi Y, Kamakura M, Murayama T, Goshima F, Kimura H, et al. Herpes simplex virus requires poly(ADP-ribose) polymerase activity for efficient replication and induces extracellular signal-related kinase-dependent phosphorylation and ICP0-dependent nuclear localization of tankyrase 1. J Virol. 2012;86(1):492–503.
23 Bamunuarachchi G, Yang X, Huang C, Liang Y, Guo Y, Liu L. MicroRNA-206 inhibits influenza A virus replication by targeting tankyrase 2. Cell Microbiol. 2021;23(2): e13281.
24 Bamunuarachchi G, Pushparaj S, Liu L. Interplay between host non-coding RNAs and influenza viruses. RNA Biol. 2021;18(5): 767–84.
25 O'Brien J, Hayder H, Zayed Y, Peng C. Overview of MicroRNA biogenesis, mechanisms of actions, and circulation. Front Endocrinol. 2018;9(402):402.
26 Makkoch J, Poomipak W, Saengchoowong S, Khongnomnan K, Praianantathavorn K, Jinato T, et al. Human microRNAs profiling in response to influenza A viruses (subtypes pH1N1, H3N2, and H5N1). Exp Biol Med. 2016;241(4):409–20.
27 Gui S, Chen X, Zhang M, Zhao F, Wan Y, Wang L, et al. Mir-302c mediates influenza A virus-induced IFNβ expression by targeting NF-κB inducing kinase. FEBS Lett. 2015; 589(24 Pt B):4112–8.
28 Zhao L, Zhu J, Zhou H, Zhao Z, Zou Z, Liu X, et al. Identification of cellular microRNA-136 as a dual regulator of RIG-I-mediated innate immunity that antagonizes H5N1 IAV replication in A549 cells. Sci Rep. 2015;5:14991.
29 Huang S-Y, Huang CH, Chen CJ, Chen TW, Lin CY, Lin YT, et al. Novel role for miR-1290 in host species specificity of influenza A virus. Mol Ther Nucleic Acids. 2019;17:10–23.
30 Zhang S, Li J, Li J, Yang Y, Kang X, Li Y, et al. Up-regulation of microRNA-203 in influenza A virus infection inhibits viral replication by targeting DR1. Sci Rep. 2018;8(1):6797.
31 Russo A, Potenza N. Antiviral effects of human microRNAs and conservation of their target sites. FEBS Lett. 2011;585(16):2551–5.
32 Umbach JL, Cullen BR. The role of RNAi and microRNAs in animal virus replication and antiviral immunity. Genes Dev. 2009;23(10): 1151–64.
33 Song L, Liu H, Gao S, Jiang W, Huang W. Cellular microRNAs inhibit replication of the H1N1 influenza A virus in infected cells. J Virol. 2010;84(17):8849–60.
34 Terrier O, Textoris J, Carron C, Marcel V, Bourdon JC, Rosa-Calatrava M. Host microRNA molecular signatures associated with human H1N1 and H3N2 influenza A viruses reveal an unanticipated antiviral activity for miR-146a. J Gen Virol. 2013;94(Pt 5):985–95.
35 Yang X, Zhao C, Bamunuarachchi G, Wang Y, Liang Y, Huang C, et al. miR-193b represses influenza A virus infection by inhibiting Wnt/β-catenin signalling. Cell Microbiol. 2019;21(5):e13001.
36 Ingle H, Kumar S, Raut AA, Mishra A, Kulkarni DD, Kameyama T, et al. The microRNA miR-485 targets host and influenza virus transcripts to regulate antiviral immunity and restrict viral replication. Sci Signal. 2015;8(406):ra126.
37 Yuva-Aydemir Y, Simkin A, Gascon E, Gao FB. MicroRNA-9: functional evolution of a conserved small regulatory RNA. RNA Biol. 2011;8(4):557–64.
38 Kozomara A, Griffiths-Jones S. miRBase: integrating microRNA annotation and deep-sequencing data. Nucleic Acids Res. 2011; 39(Database issue):D152–7.
39 Bazzoni F, Rossato M, Fabbri M, Gaudiosi D, Mirolo M, Mori L, et al. Induction and regulatory function of miR-9 in human monocytes and neutrophils exposed to proinflammatory signals. Proc Natl Acad Sci U S A. 2009;106(13):5282–7.
40 Zhang H, Chang Y, Zhang L, Kim SN, Otaegi G, Zhang Z, et al. Upregulation of MicroRNA miR-9 is associated with microcephaly and Zika virus infection in mice. Mol Neurobiol. 2019;56(6):4072–85.
41 Dong C, Sun X, Guan Z, Zhang M, Duan M. Modulation of influenza A virus replication by microRNA-9 through targeting MCPIP1. J Med Virol. 2017;89(1):41–8.
42 Ehrhardt C, Seyer R, Hrincius ER, Eierhoff T, Wolff T, Ludwig S. Interplay between influenza A virus and the innate immune signaling. Microbes Infect. 2010;12(1):81–7.
43 Crotta S, Davidson S, Mahlakoiv T, Desmet CJ, Buckwalter MR, Albert ML, et al. Type I and type III interferons drive redundant amplification loops to induce a transcriptional signature in influenza-infected airway epithelia. PLoS Pathog. 2013;9(11):e1003773.
44 Forster SC, Tate MD, Hertzog PJ. MicroRNA as type I interferon-regulated transcripts and modulators of the innate immune response. Front Immunol. 2015;6:334.
45 Pedersen IM, Cheng G, Wieland S, Volinia S, Croce CM, Chisari FV, et al. Interferon modulation of cellular microRNAs as an antiviral mechanism. Nature. 2007;449(7164):919–22.

46 Huang C, Xiao X, Yang Y, Mishra A, Liang Y, Zeng X, et al. MicroRNA-101 attenuates pulmonary fibrosis by inhibiting fibroblast proliferation and activation. J Biol Chem. 2017;292(40):16420–39.
47 Bhardwaj A, Yang Y, Ueberheide B, Smith S. Whole proteome analysis of human tankyrase knockout cells reveals targets of tankyrase-mediated degradation. Nat Commun. 2017;8(1):2214.
48 Baer A, Kehn-Hall K. Viral concentration determination through plaque assays: using traditional and novel overlay systems. J Vis Exp. 2014(93):e52065.
49 More S, Yang X, Zhu Z, Bamunuarachchi G, Guo Y, Huang C, et al. Regulation of influenza virus replication by Wnt/β-catenin signaling. PLoS One. 2018;13(1):e0191010.
50 Lam JKW, Chow MYT, Zhang Y, Leung SWS. siRNA versus miRNA as therapeutics for gene silencing. Mol Ther Nucleic Acids. 2015;4(9):e252.
51 Xu Y-R, Shi ML, Zhang Y, Kong N, Wang C, Xiao YF, et al. Tankyrases inhibit innate antiviral response by PARylating VISA/MAVS and priming it for RNF146-mediated ubiquitination and degradation. Proc Natl Acad Sci U S A. 2022;119(26):e2122805119.
52 Emeny JM, Morgan MJ. Regulation of the interferon system: evidence that Vero cells have a genetic defect in interferon production. J Gen Virol. 1979;43(1):247–52.
53 Yang N. An overview of viral and nonviral delivery systems for microRNA. Int J Pharm Investig. 2015;5(4):179–81.
54 Herrera-Carrillo E, Liu YP, Berkhout B. Improving miRNA delivery by optimizing miRNA expression cassettes in diverse virus vectors. Hum Gene Ther Methods. 2017;28(4):177–90.
55 Toots M, Plemper RK. Next-generation direct-acting influenza therapeutics. Transl Res. 2020;220:33–42.
56 Govorkova EA, McCullers JA. Therapeutics against influenza. Curr Top Microbiol Immunol. 2013;370:273–300.
57 Daugherty MD, Young JM, Kerns JA, Malik HS. Rapid evolution of PARP genes suggests a broad role for ADP-ribosylation in host-virus conflicts. PLoS Genet. 2014;10(5):e1004403.
58 Grunewald ME, Chen Y, Kuny C, Maejima T, Lease R, Ferraris D, et al. The coronavirus macrodomain is required to prevent PARP-mediated inhibition of virus replication and enhancement of IFN expression. PLoS Pathog. 2019;15(5):e1007756.
59 Liu CH, Zhou L, Chen G, Krug RM. Battle between influenza A virus and a newly identified antiviral activity of the PARP-containing ZAPL protein. Proc Natl Acad Sci U S A. 2015;112(45):14048–53.
60 Westera L, Jennings AM, Maamary J, Schwemmle M, García-Sastre A, Bortz E. Poly-ADP Ribosyl Polymerase 1 (PARP1) regulates influenza A virus polymerase. Adv Virol. 2019;2019:8512363.
61 Guo L-M, Pu Y, Han Z, Liu T, Li YX, Liu M, et al. MicroRNA-9 inhibits ovarian cancer cell growth through regulation of NF-kappaB1. FEBS J. 2009;276(19):5537–46.
62 Wei L, SandbulteMR, ThomasPG, WebbyRJ, HomayouniR, PfefferLM. NFκB negatively regulates interferon-induced gene expression and anti-influenza activity. J Biol Chem. 2006; 281(17):11678–84.
63 Yang L, Niu F, Yao H, Liao K, Chen X, Kook Y, et al. Exosomal miR-9 released from HIV tat stimulated astrocytes mediates microglial migration. J Neuroimmune Pharmacol. 2018;13(3):330–44.
64 Park S, Eom K, Kim J, Bang H, Wang HY, Ahn S, et al. MiR-9, miR-21, and miR-155 as potential biomarkers for HPV positive and negative cervical cancer. BMC Cancer. 2017;17(1):658.
65 Huang SM, Mishina YM, Liu S, Cheung A, Stegmeier F, Michaud GA, et al. Tankyrase inhibition stabilizes axin and antagonizes Wnt signalling. Nature. 2009;461(7264):614–20.
66 Guo Y, Bamunuarachchi G, Vaddadi K, Zhu Z, Gandikota C, Ahmed K, et al. Axin1: a novel scaffold protein joins the antiviral network of interferon. Mol Microbiol. 2022;118(6):731–43.